International Journal of Chemical, Materials and Biomolecular Sciences
ISSN: 2415-6620
Vol:7, No:9, 2013

# TBC for Protection of Al Alloy Aerospace Component

P. Niranatlumpong, H. Koiprasert, C. Sukhonket, K. Ninon, and N. Coompreedee

***Abstract*—**The use of a conventional air plasma-sprayed thermal barrier coating (TBC) and a porous, functionally graded TBC as a thermal insulator for Al7075 alloy was explored. A quench test at 1200°C employing fast heating and cooling rates was setup to represent a dynamic thermal condition of an aerospace component. During the test, coated samples were subjected the ambient temperature of 1200°C for a very short time. This was followed by a rapid drop in temperature resulting in cracking of the coatings. For the conventional TBC, it was found that the temperature of the Al7075 substrate decreases with the increase in the $ZrO_2$ topcoat thickness. However, at the topcoat thickness of 1100µm, large horizontal cracks can be observed in the topcoat and at the topcoat thickness of 1600µm, the topcoat delaminate during cooling after the quench test. The porous, functionally graded TBC with 600µm thick topcoat, on the other hand, was found to be as effective at reducing the substrate temperature as the conventional TBC with 1100µm thick topcoat. The maximum substrate temperature is about 213°C for the former and 208°C for the latter when a heating rate of 38°C/s was used. When the quench tests were conducted with a faster heating rate of 128°C/s, the Al7075 substrate heat up faster with a reduction in the maximum substrate temperatures. The substrate temperatures dropped from 297 to 212°C for the conventional TBC and from 213 to 155°C for the porous TBC, both with 600µm thick topcoat. Segmentation cracks were observed in both coating after the quench test.

***Keywords*—**Thermal barrier coating, Al7075, porous TBC, Quenching.

## I. Introduction

ALLOYS have been a preferred choice of material in aerospace structural applications due to their distinct properties, in particular their low density and high strength-to-weight ratio. Al alloys are also relatively cheap and readily available. Al alloys possess relatively low melting points which allow easy fabrications of components [1]-[4]. The same intrinsic property, however, limits the operating temperature of said components to just over a hundred degree Celsius. At the same time, aerospace applications become more demanding. Higher strength, fatigue resistance and operating temperature are required of the materials. Heat treated Zn-based Al7075 is one of the stronger Al wrought alloy and is widely used in aerospace applications. Al7075 starts to melt at a relatively low temperature of approximately 477°C (solidus). In order to use this material at high temperature, a thermal insulating surface may be applied.

P. Niranatlumpong , H. Koipraser, C. Sukhonket and K. Ninon are with the National Metal and Materials Technology Center,Thailand Science Park, Pathumthani, Thailand

N. Coompreedee is with the Defence Technology Institute, Ministry of Defence, Office of the Permanent Secretary of Defence Building, Nonthaburi, Thailand (e-mail: nuttapatie@hotmail.com).

This project concerns the application of a thermal barrier coating (TBC) on the outer surface of an aerospace component traveling at and beyond the speed of sound. The relative velocity at which the component cuts through the atmosphere causes frictional heating on the surface with the temperature able to reach well above 1,000°C, inevitably resulting in the partial melting of the Al-alloy component. An adequate insulating layer is therefore of utmost importance in this application. However, the Al component will be at this extreme temperature for only a few second when the component travels at its highest speed during the take-off. As soon as the velocity drops, the surface temperature also drops rapidly. Due to the dynamic thermal state and the short duration at high temperature, the component does not require as much thermal insulation as if it is in a steady state.

A material with high insulating property can be used in order to significantly reduce the working temperature of the Al alloy. A ceramic material, namely $ZrO_2$-$Y_2O_3$, is an engineering ceramic widely employed as an insulating layer in high temperature applications such as gas turbine parts due to its low thermal conductivity. Plasma spraying [5] is chosen as the coating fabrication method. A plasma sprayed $ZrO_2$-$Y_2O_3$ may exhibit a reduction in the thermal conductivity depending on its microstructure, possibly to as low as 0.6 to 1.0 W/mK at 100°C. The reduction in the thermal conductivity is mostly due to the cracks and pores typically present in the as-sprayed coating. The size and shape of these defects govern the heat transfer rate through the coating [6]-[9]. Other factors such as the coating thickness and the ambient temperature dictates the maximum temperature the Al alloy must endure.

Nevertheless, the application of a $ZrO_2$ layer with its low thermal expansion coefficient onto an Al alloy substrate with twice as high thermal expansion coefficient would expectedly cause a delamination of the coating during the sudden change in temperature. This delamination is more likely in a thicker plasma-sprayed $ZrO_2$ coating due to higher residual stress induced during processing [10]. The use of a Ni-based bondcoat layer is necessary in order to reduce the thermal expansion mismatch stress. However, in order to significantly reduce the temperature of the Al alloy substrate from an atmosphere of over 1000°C, $ZrO_2$ with a high thickness is required. Alternatively, $ZrO_2$ with higher porosity has been shown to be able to lower the thermal conductivity of the coating further [11]-[14]. Thus, the thickness of the $ZrO_2$ coating can be reduced according to R=h/K, where R is the thermal resistance, h is the thickness of the coating and K is the thermal conductivity of the coating.

Also, in order to reduce the risk of coating delamination, a graded coating where extra layers consisting of a mixture of bondcoat and topcoat can be applied in between the bondcoat

and the $ZrO_2$ topcoat. This is known as "functionally graded coating" and has been shown to be able to improve the coating adhesion [15], [16].

The objective of this work is to study the possibility of using the plasma sprayed $ZrO_2$-8%$Y_2O_3$ coating as a thermal barrier for an Al alloy 7075 subjected to high temperature and rapid temperature change. This work compares the performances of two coatings which are a conventional TBC and a functionally graded porous TBC.

## II. Experimental Procedure

### A. Coating Materials

Two types of coating material were used in this work, which are NiCrAlY as a bondcoat material and partially-stabilized $ZrO_2$ as a topcoat material. The powder details are shown in Table I.

TABLE I
Material Chemical Composition

| Material | Chemical Composition (wt.%) | Trade name | Particle size (µm) |
|---|---|---|---|
| NiCrAlY | Ni (bal) 25Cr 6Al 0.4Y | Amdry 963 | 45-75 |
| $ZrO_2$ | $ZrO_2$ (bal) 8$Y_2O_3$ | Metco 204B-NS | 45-75 |

Four groups of samples were studied in this work, see Table II. The first 3 groups, namely TC600, TC1100 and TC1600, are conventional duplex TBCs consisting of NiCrAlY bondcoat and $ZrO_2$ topcoat of varying thickness. The forth group, FG_TC600, is a TC600 sample with an addition of a graded 50 NiCrAlY /50 ZrO2 layer

### B. Substrate Preparation

Sample substrates were prepared from Al7075 sheet of 5 mm thickness. The chemical composition of Al7075 is Al (bal.) 5.1-6.1Zn 2.1-2.9Mg 1.2-2.0Cu (wt.%). The substrate dimension is 25.4mm diameter and 5 mm thickness. The samples were grit blasted prior to the plasma spraying process using 740µm alumina grit (mesh size 24) and an air pressure of 5.25 bar. The sample surface roughness achieved was approximately 9.5µm Ra.

TABLE II
Sample Designations

| Sample | Description | $ZrO_2$ thickness |
|---|---|---|
| TC_600 | NiCrAlY bondcoat + $ZrO_2$ topcoat | 600µm |
| TC_1100 | | 1100µm |
| TC_1600 | | 1600µm |
| FG_TC600 | NiCrAlY bondcoat + 50 NiCrAlY /50 $ZrO_2$ graded layer + $ZrO_2$ Topcoat (600µm thick) | |

### C. Plasma Spraying Procedure

Plasma spraying was carried out using Metco 3MBII plasma gun fitted with a 532B nozzle and a 3M210 powder injector. The powder injector was positioned externally at 90° to the plasma jet axis. The spraying parameters are shown in Table III.

TABLE III
Plasma Spraying Parameters

| Plasma Spray Parameters | NiCrAlY and Graded layer | $ZrO_2$ Topcoat |
|---|---|---|
| $N_2$ Pressure (psi) | 100 | 100 |
| $N_2$ Flow (SCFH) | 100 | 100 |
| $H_2$ Pressure (psi) | 50 | 50 |
| $H_2$ Flow (SCFH) | 15 | 15 |
| Hopper Pressure(psi) | 80 | 80 |
| Ampere (A) | 500 | 500 |
| Voltage (V) | 70-80 | 65-70 |
| Spray Rate (g/min) | 55 | 45 |
| Spray Distance (mm) | 125 | 76.2 |
| Maximum substrate temperature (°C) | ≤ 200 for TC600,TC1100,TC1600<br>≤ 140 for FG_TC600 | |

### D. Coating Characterization

The as-sprayed samples were cross-sectioned and their microstructures were observed using a scanning electron microscope (SEM). The porosity was measured using an Image Pro Plus program. ASTM C633 pull-off tensile testing was used to study the adhesion of the coatings.

### E. Quench Test

Quench test was carried out using an air/acetylene torch as a heat source. The schematic diagram is shown in Fig. 1. Fast heating and cooling rates were controlled by the speed of the torch moving in and out from the sample surface. The sample was fitted into a slot in a refractory brick in order to reduce the heat convection from the front of the coating to the Al7075 substrate. Type R thermocouples were positioned at the front adjacent to the coated surface for a measurement of the ambient temperature and at the back of the sample for the measurement of the substrate temperature. During the test, the flame torch moved in to stop at a 175mm distance from the coated surface causing the ambient temperature to rapidly rise. As soon as the ambient temperature reached 1200°C, the torch was withdrawn resulting in a sharp temperature drop. In this work, 2 heating rates of 38 and 128°C/s were used.

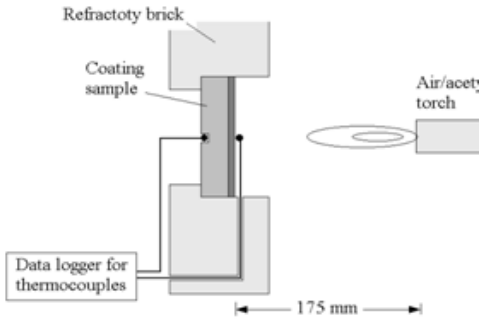


Fig. 1 Experimental setup for quench tests

## III. Results and Discussion

### A. Conventional TBC

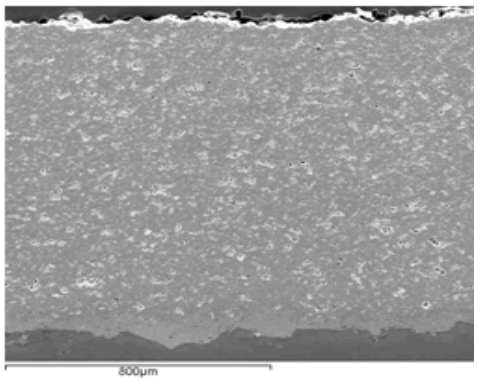


Fig. 2 SEM micrograph of a cross section of TC1100

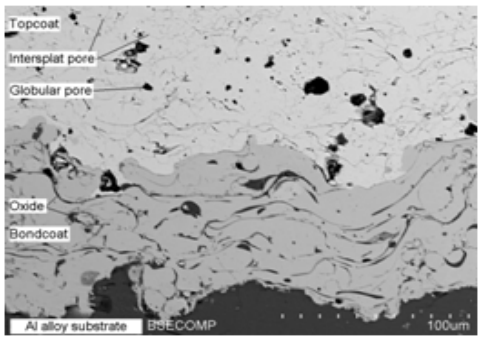


Fig. 3 SEM micrograph of a cross section of TC600

Fig. 2 and 3 reveal the typical microstructure of the plasma-sprayed $ZrO_2$ coating observed in samples TC600, TC1100 and TC1600. The coating shows a rough substrate interface from the grit blasting process without any large embedded grit. No interfacial cracks and no large cracks in the $ZrO_2$ coating can be observed. Microcracks can be seen inside the $ZrO_2$ splat. Inter-splat pores and globular pores are present within the $ZrO_2$ topcoat.

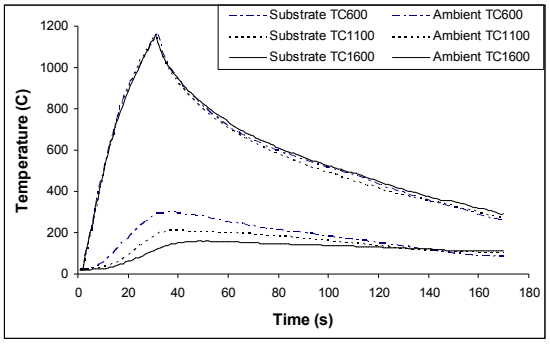


Fig. 4 Graph showing effect of the topcoat thickness on the temperature of the Al alloy substrate. The heating rate is 38°C/s

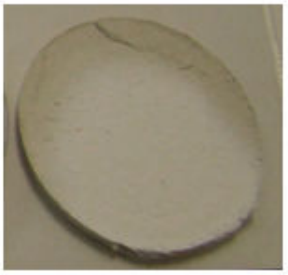

Fig. 5 Underside of the delaminated coating from sample TC1600

The coated samples in the TC series were tested using the quench test setup as shown in Fig. 1. The heating rate was controlled by the speed of the torch moving towards the sample.

At the moderate heating rate of about 38°C/s, as the thickness of the $ZrO_2$ topcoat increases, the maximum substrate temperature predictably decreases. At the topcoat thickness of 1600µm (sample TC1600), the maximum temperature of the Al alloy was reduced to approximately 159°C compared to 208 and 297°C for sample TC1100 and TC600, respectively, see Fig. 4. The TC1600 coating, however, completely delaminated after cooling when it reached the room temperature. Large cracks developed during cooling may alter the heat transfer to the substrate. The inspection of the underside of the delaminated $ZrO_2$ coating shows that the delamination took place within the $ZrO_2$ coating near the bondcoat/topcoat interface, see Fig. 5. Some large horizontal cracks can also be observed at the sample edges in some of the TC1100 samples, although the cracks did not propagate extensively enough to cause the complete delamination of the coating as in TC1600. The $ZrO_2$ coating thickness of greater than 1100µm is therefore too large to endure the 1200°C quenching.

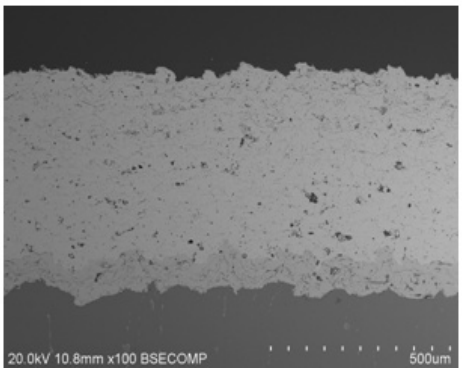


Fig. 6 As-sprayed TC600 sample in backscattered SEM mode

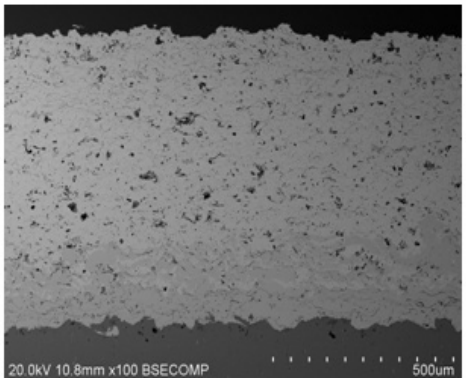


Fig. 7 As-sprayed FG_TC600 sample in backscattered SEM mode

*B. Comparison between Conventional and Functionally Graded TBCs*

The porous, functionally graded $ZrO_2$ coating was thus introduced as an alternative to the thick $ZrO_2$ in order to further reduce the temperature of the Al alloy substrate.

Fig. 6 and 7 compare the microstructures of TC600 and FG_TC600 samples in the as-sprayed condition. The 50NiCrAlY/50$ZrO_2$ graded layer is clearly visible between the bondcoat and the $ZrO_2$ coating with no cracks on either interface. FG_TC600 contains a larger average percentage of porosity than TC600. The porosity result is shown in Table IV. The difference in the amount of porosity is due to the plasma spraying process. More air cooling was used in the production of FG_TC600 in order to maintain the substrate temperature below 140°C, resulting in the higher porosity.

The adhesion strengths of the coatings were tested according to ASTM C633 and the result is shown in Table IV. The adhesion strength of FG_TC600 is 32.1 MPa compared to 27.5 Mpa for TC600. These values are lower than results from previous studies where tests were carried out mostly on Ni-alloy substrate [17]-[19] due to a residual thermal stress induced during the plasma-spraying process as a result of a larger thermal expansion mismatch between the ceramic coating and the Al alloy substrate. The adhesion strength of FG_TC600 is notably higher than that of TC600. This is because the material gradation leads to a change in the thermal stress, thus, reducing the thermal stress at critical locations [20].

TABLE IV
COATING POROSITY AND ADHESION STRENGTH

| As-sprayed sample | TC600 | FG_TC600 |
|---|---|---|
| Average porosity (%) | 6.5 | 8.6 |
| Adhesion strength (Mpa) | 27.5 | 32.1 |

The functionally graded bondcoat adds about 100µm of 50NiCrAlY/50$ZrO_2$ mixture to the total thickness of the coating which inevitably affects the heat transfer rate of the coating. The higher porosity level in FG_TC600 is another factor affecting the thermal conductivity of the coating. Fig. 8 shows that both the intersplat (or lamellar) and the globular porosities are higher in FG_TC600 compared to TC600. Previous works have shown that the intersplat porosity plays a significant role in lowering the thermal conductivity of the plasma-sprayed $ZrO_2$ coating [21], [13].

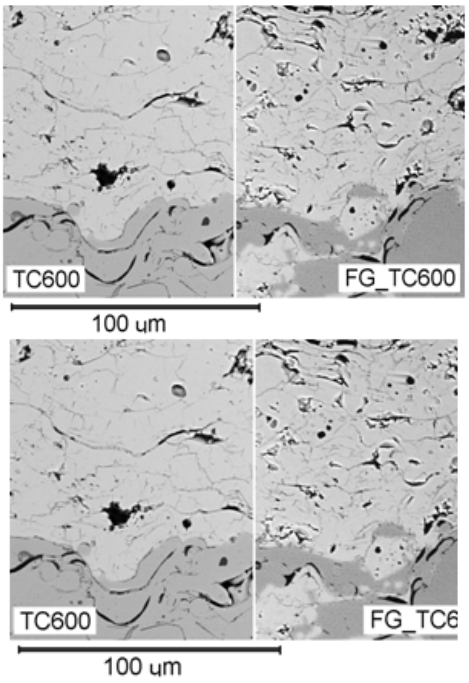


Fig. 8 Backscattered SEM micrographs comparing porosity in TC600 and FG_TC600

The porous FG_TC600 coating proves to be effective at lowering the substrate temperature at a moderate heating rate of about 38°C/s. The maximum substrate temperature is about 213°C which is comparable to that of TC1100 at 208°C and is significantly lower than that of TC600 at 297°C, see Fig. 4 and 9.

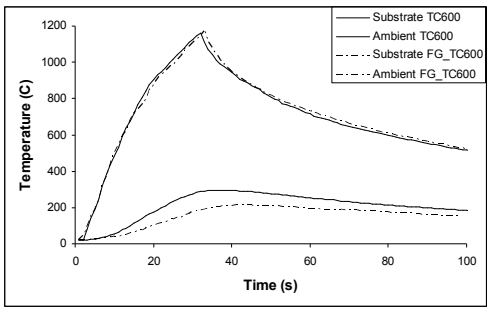


Fig. 9 Graph showing the effect of high porosity and functionally graded bondcoat on the temperature of the Al alloy substrate. The heating rate is 38°C/s

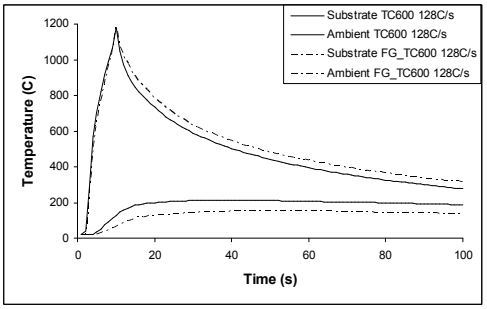


Fig. 10 Graph showing the effect of high porosity and functionally graded bondcoat on the temperature of the Al alloy substrate. The heating rate is 128°C/s

Increasing the heating rate in the quench test results in a lower maximum substrate temperature. Fig. 9 and 10 show that for both TC600 and FG_TC600, the substrates heat up faster in response to the heating rate of 128°C/s while the maximum substrate temperatures drop from 297 to 212°C for TC600 and from 213 to 155°C for FG_TC600. Both coatings were still intact after quenching. No large horizontal cracks can be observed.

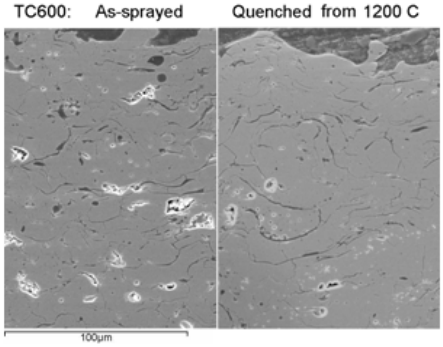


Fig. 11 Micrographs of TC600 cross-sections before and after quenching test using the heating rate of 128°C/s

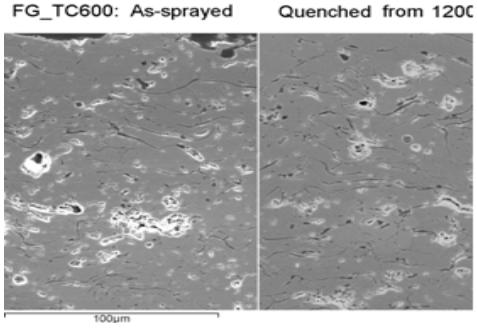


Fig. 12 Micrographs of FG_TC600 cross-sections before and after quenching test using the heating rate of 128°C/s

Fig. 11 and 12 reveal the cross-sections of the coatings before and after the quenching test. There are no significant changes in the structures. No quantifiable evidence of sintering resulting in denser coating can be observed because the coatings were at high temperature for a very short time.

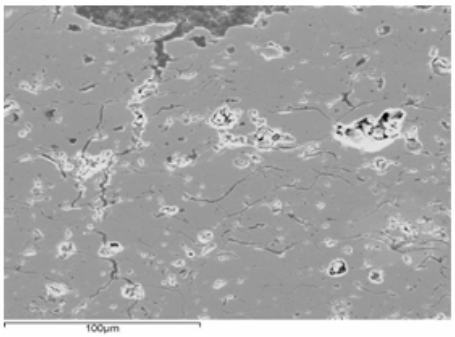


Fig. 13 Micrograph of FG_TC600 cross-section after quenching test using the heating rate of 128°C/s, showing a segmentation crack

The major change in the microstructures after quenching is the presence of large vertical segmentation cracks in both coatings subjected to the heating rate of 128°C/s, see Fig. 13. The segmentation cracks travel along the intersplat pores and the microcracks contained within the splats. In order to quantify the damage, vertical cracks of length greater than 50 µm within 5000µm width of the coating cross sections were measured on one sample from each group of samples. It was found that there are similar crack densities, 10 and 11 cracks per 5000µm width for TC600 and FG_TC600 respectively. The crack length, however, is significantly longer in FG_TC600. The average crack lengths are 115 and 175µm for TC600 and FG_TC600 respectively. These values have a large error however due to the following limitations in measurement;

1. The downward crack paths are non-linear but only the vertical distances were measured.
2. Shorter and smaller cracks cannot be easily differentiated from the pre-existing intersplat pores and lamellar microcracks, thus cracks shorter than 50 µm were not included in the measurement.

Therefore, these numerical data can serve only as a comparison, indicating that FG_TC600 contains larger segmentation cracks than TC600 after the quench test. This can be explained in terms of the difference in the contraction strain between the two groups of sample.

TABLE V
THERMAL EXPANSION COEFFICIENTS OF THE SAMPLE MATERIALS

| | **Al 7075** | **APS $ZrO_2$-$Y_2O_3$** |
|---|---|---|
| CTE x$10^{-6}$ ($K^{-1}$) | 23.2 | 10 |

APS = Air plasma sprayed coating

As the sample was cooled approaching room temperature, the sample was subjected to a contraction stress. The linear contraction strain, $\frac{\Delta L}{L}$, can be describe as;

$$\frac{\Delta L}{L} = \alpha_L \Delta T \quad (1)$$

where $\alpha_L$ is the linear thermal expansion coefficient, and $\Delta T$ is the change in temperature. Using the thermal properties in Table V and data from Fig. 10, the contraction strain of the samples can be calculated, see Table VI. The strain is much greater in the $ZrO_2$ topcoat compared to the Al7075 substrate due to a larger change in temperature even though the linear thermal expansion coefficient is less than half that of the Al alloy substrate. As the sample was allowed to contract during cooling, the change in dimension of the Al7075 relieved some but not all of the stress in the topcoat. TC600 was subjected to a higher substrate temperature during quench test than FG_TC600, thus it was put under a larger contraction, which in turn, was able to relieve more stress in the $ZrO_2$ topcoat. Thus, FG_TC600 was left with a larger residual stress than TC600 resulting in larger segmentation cracks as stress was relieved.

TABLE VI
RESIDUAL STRAIN IN $ZrO_2$ TOPCOAT

| | Strain in $ZrO_2$ | Strain in Al7075 |
|---|---|---|
| TC600 | $1.2x10^{-2}$ | $4.3x10^{-3}$ |
| FG_TC600 | $1.2x10^{-2}$ | $3x10^{-3}$ |

Vertical segmentation cracks have been reported to increase the strain tolerance of the ceramic coating, although it also reduces the effectiveness of the coating as a thermal barrier due to the increase in the thermal conductivity of the coating [13], [14].

## IV. CONCLUSION

In this paper, the possibility of using TBC as an insulator for Al7075 at 1200°C under a rapid increase and decrease in temperature was explored. The work compared a conventional TBC with a more porous, functionally graded coating. The results can be summarized as followed;

The conventional TBC is effective at reducing the substrate temperature during the quench test from 1200°C. However, as the thickness of $ZrO_2$ topcoat increases, even though the substrate temperature can be reduced further, delamination cracks starts to form in the topcoat at the thickness of 1100 µm.

The porous, functionally graded TBC is more effective as a thermal insulator than the conventional TBC of the same thickness due to the higher porosity in the $ZrO_2$ structure. When a heating rate of about 38°C/s was used, the maximum substrate temperature of the 600µm thick porous TBC (FG_TC600) was comparable to that of the 1100µm thick conventional TBC (TC1100).

The Al7075 substrate temperature was about 213°C for the former and 208°C for the latter.

After the quench test, both groups of sample exhibit segmentation cracking in the $ZrO_2$ topcoat. The cracks are longer in the porous TBC due to the lower substrate temperature resulting in less thermal stress and less contraction in the substrate. This also means less stress relief for the $ZrO_2$ topcoat, hence the segmentation cracking is more severe than in the conventional TBC.

## REFERENCES

[1] P. E. Magnusen, R. J. Bucci, A. J. Hinkle, J. R. Brockenbrough and H. J. Konish, "Analysis and prediction of microstructural effects on long-term fatigue performance of an aluminum aerospace alloy", Int. J. Fatigue Vol. 19, (1997) S275–S283.

[2] M. S. Kenevisi, S. M. Mousavi Khoie, "An investigation on microstructure and mechanical properties of Al7075 to Ti–6Al–4V Transient Liquid Phase (TLP) bonded joint", Materials and Design 38 (2012) 19–25.

[3] J. Ren, Y. Li and T. Feng, "Microstructure characteristics in the interface zone of Ti/Al diffusion bonding", Materials Letters, Volume 56, Issue 5, (2002) 647-652.

[4] K. Dehghani, A. Nekahi, M. Ali and M. Mirzaie, "Optimizing the bake hardening behavior of Al7075 using response surface methodology", Materials and Design 31 (2010) 1768–1775.

[5] R. McPherson, "A review of microstructure and properties of plasma sprayed ceramic coatings", Surface and Coatings Technology, Volumes 39–40, Part 1, (1989) 173-181.

[6] P. G. Klemens, M. Gell, "Thermal conductivity of thermal barrier coatings", Materials Science and Engineering A245 (1998) 143–149.

[7] F. Cernuschi, S. Ahmaniemi, P. Vuoristo, T. Mäntylä, "Modelling of thermal conductivity of porous materials: application to thick thermal barrier coatings", Journal of the European Ceramic Society, Volume 24, Issue 9, (2004) 2657-2667.

[8] H. Zhao, F. Yu, T.D. Bennett and H. N. G. Wadley, "Morphology and thermal conductivity of yttria-stabilized zirconia coatings", Acta Materialia, Volume 54, Issue 19, (2006) 5195-5207.

[9] J. Zhang, V. Desai, "Determining thermal conductivity of plasma sprayed TBC by electrochemical impedance spectroscopy", Surface and Coatings Technology, Volume 190, Issue 1, ( 2005) 90-97

[10] E. F. Rejda, D. F. Socie and T. Itoh, "Deformation behavior of plasma-sprayed thick thermal barrier coatings", Surface and Coatings Technology 113 (1999) 218–226.

[11] S. Ahmaniemi, P. Vuoristo, T. Mantyla, C. Gualco, A. Bonadei, R. Di Maggio, "Thermal cycling resistance of modified thick thermal barrier coatings", Surface & Coatings Technology 190 (2005) 378– 387.

[12] F. Cernuschi, S. Ahmaniemi, P. Vuoristo, T. Mantyla, "Modelling of thermal conductivity of porous materials: application to thick thermal barrier coatings", Journal of the European Ceramic Society 24 (2004) 2657–2667.

[13] A. Kulkarni, A. Vaidya, A. Goland, S. Sampath, H. Herman, "Processing effects on porosity-property correlations in plasma sprayed yttria-stabilized zirconia coatings", Materials and Engineering A359 (2003) 100-111.

[14] S. Ahmaniemi, P. Vuoristo, T. Mantyla, F. Cernuschi, L. Lorenzoni, "Modified thick thermal barrier coatings: Thermophysical characterization", Journal of the European Ceramic Society 24 (2004) 2669–2679.

[15] A. M. Khoddami, A. Sabour, S. M. M. Hadavi, "Microstructure formation in thermally-sprayed duplex and functionally graded NiCrAlY/Yttria-Stabilized Zirconia coatings", Surface & Coatings Technology 201 (2007) 6019–6024.

[16] Z. L. Dong, K. A. Khor, Y. W. Gu, "Microstructure formation in plasma-sprayed functionally graded NiCoCrAlY/yttria-stabilized zirconia coatings", Surface and Coatings Technology 114 (1999) 181–186.

[17] N. R. Shankar, C. C. Berndt and H. Herman, "Failure And Acoustic Emission Response Of Plasma Sprayed ZrO2-8wt.%Y2O3", Ceram.Eng.Sci.Proc., 3[9-10] (1982) 772-792.

[18] K. A. Khor, Z. L. Dong and Y. W. Gu, "Influence of oxide mixtures on mechanical properties of plasma sprayed functionally graded coating", Thin Solid Films, Volume 368, Issue 1, ( 2000) 86-92.

[19] W. Shen, F. C. Wang, Q. B. Fan, Z. Ma, X. W. Yang, "Finite element simulation of tensile bond strength of atmospheric plasma spraying thermal barrier coatings", Surface and Coatings Technology, Volume 205, Issues 8–9 ( 2011) 2964–2969.

[20] O. Bleeck, D. Munz, W. Schaller and Y. Y Yang, "Effect of a graded interlayer on the stress intensity factor of cracks in a joint under thermal loading", Engineering Fracture Mechanics, Volume 60, Issues 5–6, (1998) 615-623.

[21] B. Ercan, K. J. Bowman, R. W. Trice, H. Wang and W. Porter, "Effect of initial powder morphology on thermal and mechanical properties of stand-alone plasma-sprayed 7 wt.% Y2O3–ZrO2 coatings", Materials Science and Engineering A 435–436 (2006) 212–220.